

Pressure-induced behavior of the hydrogen-dominant compound $\text{SiH}_4(\text{H}_2)_2$ from first-principles calculations

Xing-Qiu Chen,¹ Shibing Wang,^{2,3} Wendy L. Mao,^{3,4,5} and C. L. Fu⁶¹*Shenyang National Laboratory for Materials Science, Institute of Metal Research, Chinese Academy of Sciences, Shenyang 110016, China*²*Department of Applied Physics, Stanford University, Stanford, California 94305, USA*³*Stanford Institute for Materials and Energy Science, SLAC National Accelerator Laboratory, Menlo Park, California 94025, USA*⁴*Department of Geological and Environmental Sciences, Stanford University, Stanford, California 94305, USA*⁵*Photon Science Department, SLAC National Accelerator Laboratory, Menlo Park, California 94025, USA*⁶*Materials Science and Technology Division, Oak Ridge National Laboratory, Oak Ridge, Tennessee 37831, USA*

(Received 24 June 2010; published 21 September 2010)

The structural and electronic properties of the high-pressure molecular compound $\text{SiH}_4(\text{H}_2)_2$ have been calculated using density-functional theory. We identify the molecular hydrogen positions within the face-centered cubic unit cell and further find that pressure-induced intermolecular interaction between SiH_4 and H_2 units plays an important role in stabilizing this new compound. The electronic structure is characterized by a wide band gap of 6.1 eV at 6.8 GPa, which closes with pressure and finally becomes metallic at 200 GPa due to electronic band overlap accompanied by a structure change. These findings have potential implications for understanding metallization and superconductivity in H_2 .

DOI: [10.1103/PhysRevB.82.104115](https://doi.org/10.1103/PhysRevB.82.104115)

PACS number(s): 64.70.kt, 31.15.A–, 62.50.–p, 81.40.Vw

I. INTRODUCTION

At high-pressure hydrogen is predicted to metallize and display novel behavior such as superconductivity, superfluidity and a quantum liquid state.^{1–5} However, the metallization of hydrogen at room temperature has not yet been observed experimentally due to the very high pressures required.^{6,7} Hydrogen-dominant solids, i.e., those containing a small amount of nonhydrogen atoms embedded in a network of hydrogen stabilized by intermolecular and intramolecular interactions, have been proposed as analog materials which may mimic the behavior of solid hydrogen at relatively lower pressure.⁸

A flurry of work on the group IV hydride SiH_4 (Refs. 9–14) has shown that metallization of a hydrogen-dominant material can be achieved at much lower pressures than for pure hydrogen. Studies by Strobel *et al.*¹⁵ and Wang *et al.*¹⁶ explored the high-pressure behavior of the even more hydrogen-rich system $\text{SiH}_4:\text{H}_2$, and found eutectic behavior at 6.1 GPa and the formation of a new compound $\text{SiH}_4(\text{H}_2)_2$ near 7 GPa. X-ray diffraction results indicate that the structure of the new compound belongs to the cubic space group $F\bar{4}3m$, however, the exact positions of the molecular hydrogen cannot be resolved experimentally. It is also unclear why the compound is stable above 6–7 GPa.

In this study, we investigated the possible hydrogen positions and analyzed the electronic structure of $\text{SiH}_4(\text{H}_2)_2$ through first-principles calculations within the framework of density-functional theory (DFT). We identified the mechanism for the stabilization of $\text{SiH}_4(\text{H}_2)_2$ under pressure as due to the enhanced intermolecular interaction. Our calculations demonstrated that this new compound is a wide gap insulator at lower pressure and undergoes band-gap closure at 200 GPa. The calculated pressure-dependent structural properties and Raman spectra shift are in good agreement with experiments. These results provide insight into the effect of pres-

sure on hydrogen-dominant materials and has implications for the metallization of pure hydrogen.

II. COMPUTATIONAL AND EXPERIMENTAL DETAILS

First-principles calculations were performed using the Vienna *ab initio* simulation package¹⁷ with the ion-electron interaction described by the projector augmented wave potential (PAW).¹⁸ The energy cutoff for the plane-wave expansion of eigenfunctions was set to 500 eV. We used the generalized-gradient approximation (GGA) based on the Perdew-Burke-Ernzerhof (PBE) scheme¹⁹ for the exchange-correlation functional. The core radii of Si and H potentials are chosen to be 2.944 Å (PAW-PBE Si 05Jan2001) and 2.174 Å (PAW-PBE H 15Jun 2001), respectively. For properties at low pressures, we also checked the plane-wave energy cutoff of 700 eV for the eigenfunctions and found the results nearly unchanged from those of 500 eV. Optimization of structural parameters was achieved by minimizing forces and stress tensors. Highly converged results were obtained utilizing a dense $11 \times 11 \times 11 \bar{k}$ -point grid for the Brillouin-zone integration. To calculate the amount of electronic charge, we used the code of Bader charge analysis including both valence and core charges²⁰ obtained within a grid of $300 \times 300 \times 300$ (27 millions grid points). This grid is dense enough to correctly reproduce the core electron charge of both Si and H atoms. For the proposed structure, Raman spectra under pressure have been calculated using QUANTUM-ESPRESSO.²¹ A series of self-consistent total-energies calculations were performed to determine the equilibrium lattice parameters within the norm-conserving pseudopotentials before conducting the Raman calculations. The experimental data in this work was collected in a diamond anvil cell. Details of the sample preparation can be found in Ref. 16. Synchrotron x-ray diffraction was carried

TABLE I. DFT optimized structural parameters at 6.8 GPa for the $F\bar{4}3m$ structure of $\text{SiH}_4(\text{H}_2)_2$. Lattice parameters are given in angstrom.

Space group	$F\bar{4}3m$
a in Å	6.279 (expt.: 6.426 ^a)
Si in $4a$ sites	(0, 0, 0)
H in $16e$ sites	(0.1348, 0.1348, 0.1348)
	Eight H-H pairs
H-H pair1	(0.5441, 0.0015, 0.9601)
H-H pair1	(0.4559, 0.0040, 0.0404)
H-H pair2	(0.9675, 0.4495, 0.9878)
H-H pair2	(0.0304, 0.5496, 0.0034)
H-H pair3	(0.0433, 0.9952, 0.5413)
H-H pair3	(0.9575, 0.9990, 0.4586)
H-H pair4	(0.4974, 0.5517, 0.5298)
H-H pair4	(0.4942, 0.4482, 0.4709)
H-H pair5	(0.2242, 0.2929, 0.7412)
H-H pair5	(0.2902, 0.2014, 0.7817)
H-H pair6	(0.7800, 0.7973, 0.7061)
H-H pair6	(0.7476, 0.7105, 0.7823)
H-H pair7	(0.2046, 0.7944, 0.2750)
H-H pair7	(0.2887, 0.7113, 0.2543)
H-H pair8	(0.7755, 0.2850, 0.2654)
H-H pair8	(0.7068, 0.2029, 0.2113)

^aReference 15.

out at HPCAT, Advanced Photon Source, Argonne National Laboratory.

III. RESULTS AND DISCUSSIONS

We performed a series of searches for the possible hydrogen positions within the face-centered cubic (fcc) $F\bar{4}3m$ space group proposed from experiments.¹⁵ The tetrahedra SiH_4 unit occupies the fcc lattice sites. The positions of eight H_2 pairs are at two nonequivalent sites. Four equivalent pairs are at the middle of each axis of the cubic structure and in the center of the cube. The other four pairs of H_2 are at the 1/4 or 3/4 position of the four-body diagonal lines forming a tetrahedron. The latter four are the nearest neighbors of a SiH_4 molecule. The optimized lattice parameters at 6.8 GPa for the lowest-energy configuration are compiled in Table I.

Figure 1 shows the calculated volumes as a function of pressure together with previous experimental results¹⁵ and our new data point. The theoretical equation of state (EOS) is consistent with the experimental findings, especially at higher pressures. Below 15 GPa, the calculated volumes are 3–6 % smaller than the corresponding experimental values. This discrepancy may be attributed to the fact that at low pressures intermolecular van der Waals interactions are dominant, given that there is a large separation between the H_2 and the SiH_4 units, and DFT methods are known to have limited accuracy describing this type of long-range interactions. Temperature may also be a source for the discrepancy

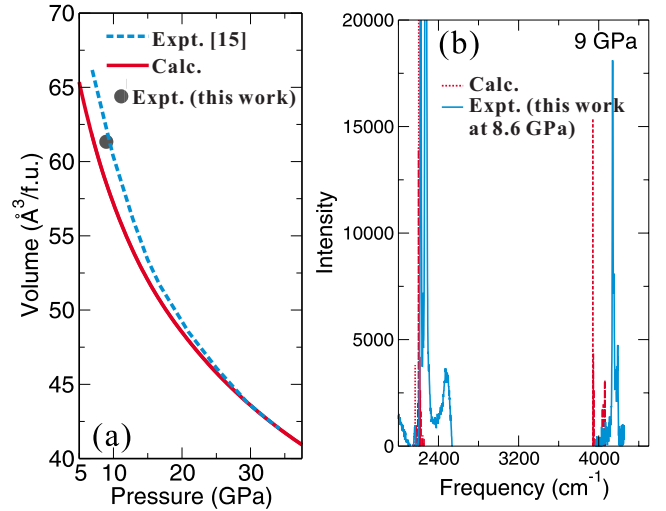


FIG. 1. (Color online) Panel (a), Comparison of the calculated pressure-dependent volumes (equation of state) with available experimental data. Panel (b), calculated and experimental Raman spectra at 9 GPa and 8.6 GPa, respectively.

in the lattice constants at low pressures. Our calculated data were performed at absolute zero temperature whereas the experimental measurements were collected at 300 K.

We derived a zero-pressure bulk modulus $K_0=5.3$ GPa with $K'=3.76$ from a fit to a third-order Birch-Murnaghan EOS, compared to the experimental values of $K_0=6.8$ GPa and $K'=4$.¹⁵

The Raman spectra of SiH_4 and H_2 can provide important information for understanding the property change in $\text{SiH}_4(\text{H}_2)_2$ under compression. A detailed description of the vibrational modes of pure H_2 and pure SiH_4 can be found in previous high pressure Raman spectroscopy work.^{13,22,23} We calculated the Raman spectra at 9 and 25 GPa. From the 9 GPa data (shown in Fig. 1), we see that the major representative experimental Raman features ($\nu_2(E)$, $\nu_1(A_1)$, and $\nu_3(F_2)$ stretching modes in SiH_4 and the H_2 vibron) have been qualitatively reproduced in our theoretical calculations, especially the multiple peaks in hydrogen vibron region. At 9 GPa, our calculations revealed that the SiH_4 $\nu_1(A_1)$ feature is at 2201 cm^{-1} , and the H_2 vibron is at 3940 cm^{-1} . Increasing pressure up to 25 GPa, their positions shift to 2412 cm^{-1} , and 3866 cm^{-1} . Comparing with the experimental measurement,¹⁵ our theoretical values are underestimated by 5–6 %. Despite the underestimation, the qualitative trend for our calculated Raman shifts with pressure are consistent with experimental observations.^{15,16} The most intense peak from the $\nu_1(A_1)$ and $\nu_3(F_2)$ stretching modes of the SiH_4 unit shows substantial blueshift with increasing pressure (Fig. 1). Conversely, the pressure-dependent vibron mode from H_2 in $\text{SiH}_4(\text{H}_2)_2$ exhibits strong redshifts. This softening becomes larger with increasing pressure. We also find that the low-frequency $\nu_2(E)$ mode (approximately 940 cm^{-1}) is insensitive to pressure. Altogether, our results indicate there are increased intermolecular interactions in $\text{SiH}_4(\text{H}_2)_2$ under pressure.

Studying the pressure-dependent electronic structures provides insight into the stabilization mechanism of the com-

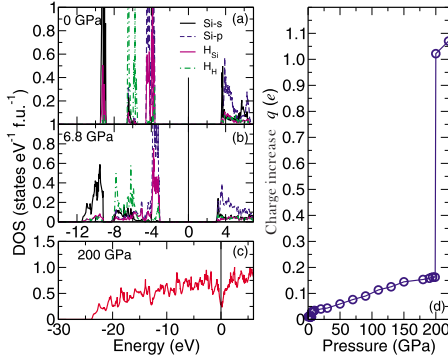


FIG. 2. (Color online) Panels (a–c): the calculated total and local DOS at three pressures of 0 GPa, 6.8 GPa, and 200 GPa, respectively. H_{Si} and H_H denote the H atom from the units of SiH_4 and H_2 molecule, respectively. The Fermi level is set to zero. Panel (d): the calculated pressure-dependent charge increase, q , for the H_2 molecules.

compound $SiH_4(H_2)_2$. Figures 2(a)–2(c) compares the calculated electronic densities of states (DOS) at 0, 6.8, and 200 GPa. The band structures that the DOS is based on was calculated according to the experimentally extracted volume¹⁵ of 410.12 \AA^3 . The 0 GPa DOS represents the simple mixed phase of SiH_4 and H_2 , where the energy level of hydrogen from SiH_4 (denoted as H_{Si}) and that of the hydrogen from H_2 (denoted as H_H) do not show any overlap significantly. As the pressure increases to 6.8 GPa, the H_{Si} and H_H energy bands start to overlap, indicating the onset of pressure-induced intermolecular interaction. By taking the superposition of the charge densities of SiH_4 and H_2 systems at the same lattice constant as the reference, we found that the interaction is manifested by charge accumulation at two sites (cf., Fig. 3): one is the interstitial space between H_{Si} and H_H , the other is on the H_{Si} site of SiH_4 . The former bridges the H_{Si} and H_H , and thus is a direct evidence of intermolecular interaction between SiH_4 and H_2 units. The effect of the latter charge accumulation may have contributed to the change in the Si-H bond strength, and therefore, the pressure-dependent Raman-spectra shift. The charge maxima between the H_{Si} and H_H atoms is consistent with the

site- l -projected density of states [Fig. 2(b)]. It is also interesting to note that the charge increase in the interstitial space does not exist below 5.4 GPa. Thus, the stabilization of the compound $SiH_4(H_2)_2$ arises from the overlapping of valence electrons in the interstitial spaces bridging the H_{Si} and H_H . The spatial overlap of the hydrogen atoms is consistent with their DOS overlap in energy as pressure changes from ambient pressure to 6.8 GPa, shown in Fig. 2(b).

$SiH_4(H_2)_2$ consists of two sublattices, one occupied by SiH_4 tetrahedra and the other by molecular H_2 pairs. To further identify the bonding character in this new compound, we calculated the amount of charge accumulations in both the unit of SiH_4 and the H_2 using the Bader technique.²⁰ Our results reveal the decrease and increase in electronic charge in the SiH_4 tetrahedra and H_2 pairs, respectively, as the pressure increases. In terms of our PAW calculations within the denser $300 \times 300 \times 300 k$ mesh (27 millions grid points), the amount of charge increase for the H_2 pair, q , as a function of pressure is displayed in Fig. 2(d). With increasing pressure, we found two obvious jumps in the curve of the pressure-dependent charge increase for the H_2 pairs. Before the first jump occurs at 5.4 GPa, there is a constant increased charge q of approximately $0.01e$. Above 5.4 GPa, the magnitude of q suddenly increases to about $0.04e$. Eventually, it reaches $0.18e$ at 199 GPa. The pressure range above 5.4 GPa agrees with the experimental region where $SiH_4(H_2)_2$ becomes stable. The likely mechanism that contributes to the increase in charge for the H_2 units above 5.4 GPa are: (1) the contraction of the hydrogen wave function more closely into the nuclei region as the bonding between H_H and H_{Si} is developed [also see Fig. 3(c)], and (2) the increase in charge transfer (or extension) from the SiH_4 tetrahedra to the H_2 units as the intermolecular distance decreases. We found that the pressure-induced charge increase (or distortion) for the hydrogen molecule has an effect on weakening the H-H bond, which results in softening of the H_2 vibron. This is similar to what has been found in pure H_2 both experimentally² and theoretically at pressures as high as 200 GPa (Ref. 24) and in the recently discovered Xe- H_2 compound.²⁵

We also observed that the charge on each H_H of H_2 is different. The nearest H_2 to SiH_4 carries a charge asymmetry between 0.02 and $0.04e$ whereas the charge asymmetry of

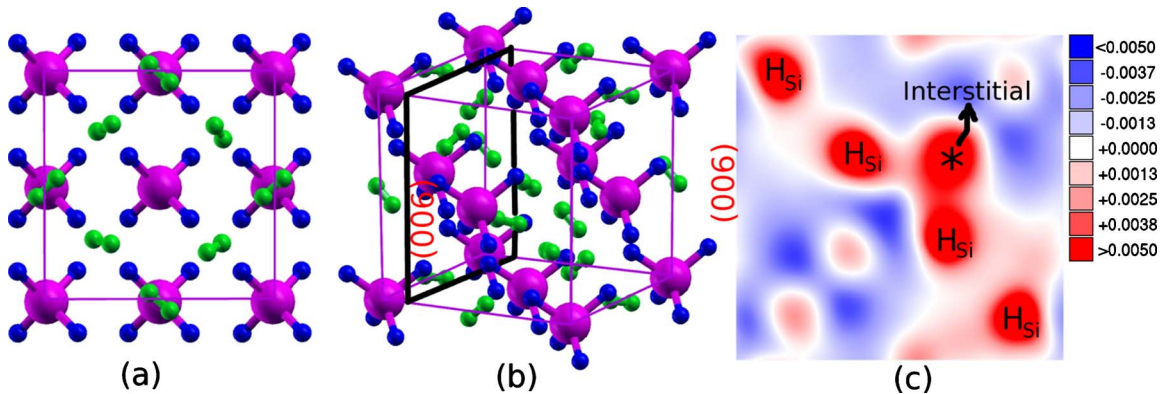


FIG. 3. (Color online) The crystal structure of $SiH_4(H_2)_2$: panel (a) two-dimensional structural projection and panel (b) a three-dimensional structure. Large and small balls denote Si and H, respectively. Panel (c): contour plot of the charge difference in the (006) plane as marked in panel (b). Positive values denotes the charge accumulation and negative value charge depletion. * marks the region of charge accumulation in the interstitial spaces.

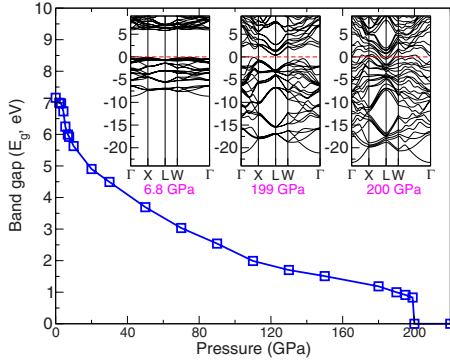


FIG. 4. (Color online) Pressure-dependent band gap sizes (E_g in electron volt) by GGA-PBE approximations. Inset from left to right: the calculated electronic-band structures at 6.8 GPa, 199 GPa, and 200 GPa, respectively. Zero-energy lines indicate the top of valence band.

the next nearest H_2 is between 0.01 and $0.02e$. Furthermore, these charge asymmetry for all H_2 pair decreases with increasing pressure, consistent with the reduced H_2 IR intensity at higher pressure observed in the $SiH_4(H_2)_2$ IR experiment.¹⁵

We also note that, after 199 GPa, charge transfer q suddenly increases to $1.02e$, accompanied by metallization of the compound. This is partly due to the change in the locations of the Si atoms from their face-centered $4a$ position, implying that the compound is in a different structure above this pressure. Also, at this high pressure, the electrons become more delocalized as evidenced in the increasingly parabolic behavior of the band dispersion. We also note that the metallization is accompanied by the occupation of antibonding orbitals.

We have calculated the electronic band structures of $SiH_4(H_2)_2$ at 0 K. The results indicate that the new compound is a transparent indirect wide-gap insulator with a large band gap of about 6.1 eV at 6.8 GPa. With increasing pressure, the gap decreases, and the dispersion of each band increases indicating an increasing intermolecular interaction. At 200 GPa, the bandgap closes and $SiH_4(H_2)_2$ becomes metallic (cf., Fig. 4) because of a structural transformation. Normally, standard density-functional theory underestimates band gap, implying the real pressure-dependent gaps are larger than predicted in our PBE-GGA approximations. Nevertheless, based on the standard DFT calculation, the predicted metallization pressure²⁶ is lower than that of pure H_2 again demonstrating that the addition of a group IV hydride can lower the metallization pressure compared to pure hydrogen. In our calculation (cf., Fig. 4) the compound has a band gap of about 4.3 eV at 35 GPa, which implies that experimentally observed sample darkening might be due to

hydrogen reaction with gasket material, a concern addressed in Ref. 15.

The metallization scheme of bandgap closure in $SiH_4(H_2)_2$ is consistent with the prediction for molecular metallic hydrogen,²⁶ and the possibility of superconductivity at relatively high temperature.²⁷ The present compound inherits many of the electronic and vibrational features of the dense solid superconducting phases of both SiH_4 (Ref. 12) and H_2 .^{8,26}

A recent publication that used GGA and GW methods to investigate the electronic structure of $SiH_4(H_2)_2$ found that the metallization occurs at 145 GPa and 160 GPa with GGA and GW methods, respectively.²⁸ The difference compared to our results might be due to the selection of potentials (Si_h and H_h). However, both theoretical investigations confirmed that at 35–50 GPa the $SiH_4(H_2)_2$ is still a wide gap insulator and that the metallization occurs at a much higher pressure via band gap closure.

IV. CONCLUSION

In summary, we have performed first-principles calculations to investigate the pressure-dependent behavior of the structural and electronic properties of the $SiH_4(H_2)_2$ and its stability mechanism. We determined the positions of the hydrogen atoms and explicitly calculated the pressure-induced charge distribution due to intermolecular interaction. Besides charge increase for the H_2 pairs, the compound is also stabilized by the charge accumulation at the interstitial position between H_{Si} from SiH_4 and H_H from H_2 . Our results are further supported by the calculated Raman spectra which are in good qualitative agreement with experimental observations. In the $SiH_4(H_2)_2$, the H_2 vibron shows substantial redshift whereas the stretching modes from SiH_4 exhibit strong blueshift with increasing pressure. We also show that the compound is a wide-gap insulator at low pressure and eventually becomes metallic above 200 GPa, accompanied by a large charge transfer from SiH_4 to H_2 during metallization.

ACKNOWLEDGMENTS

We thank Timothy Strobel for helpful discussions. Research at the Shengyang National Laboratory for Materials Science (X.-Q.C.) was supported by the Materials Processing Modeling Division and by the “Hundred Talents Project” of Chinese Academy of Science. Research at Oak Ridge National Laboratory (C.L.F.) was supported by the U.S. Department of Energy, Office of Basic Energy Sciences, Materials Sciences and Engineering Division. S.W. and W.L.M. are supported by the U.S. Department of Energy through the Stanford Institute for Materials and Energy Science (Grant No. DE-AC02-76SF00515).

- ¹N. W. Ashcroft, *Phys. Rev. Lett.* **21**, 1748 (1968).
- ²H. K. Mao and R. J. Hemley, *Rev. Mod. Phys.* **66**, 671 (1994).
- ³E. Babaev, A. Sudbo, and N. W. Ashcroft, *Nature (London)* **431**, 666 (2004).
- ⁴S. A. Bonev, E. Schwegler, T. Ogitsu, and G. A. Galli, *Nature (London)* **431**, 669 (2004).
- ⁵P. Tolédano, H. Katzke, A. F. Goncharov, and R. J. Hemley, *Phys. Rev. Lett.* **103**, 105301 (2009).
- ⁶S. T. Weir, A. C. Mitchell, and W. J. Nellis, *Phys. Rev. Lett.* **76**, 1860 (1996).
- ⁷C. Narayana, H. Luo, J. Orloff, and A. L. Ruoff, *Nature (London)* **393**, 46 (1998).
- ⁸N. W. Ashcroft, *Phys. Rev. Lett.* **92**, 187002 (2004).
- ⁹J. Feng, W. Grochala, T. Jaroń, R. Hoffmann, A. Bergara, and N. W. Ashcroft, *Phys. Rev. Lett.* **96**, 017006 (2006).
- ¹⁰C. J. Pickard and R. J. Needs, *Phys. Rev. Lett.* **97**, 045504 (2006).
- ¹¹D. Y. Kim, R. H. Scheicher, S. Lebégue, J. Prasongkit, B. Arnaud, M. Alouani, and R. Ahuja, *Proc. Natl. Acad. Sci. U.S.A.* **105**, 16454 (2008).
- ¹²M. I. Eremets, I. A. Trojan, S. A. Medvedev, J. S. Tse, and Y. Yao, *Science* **319**, 1506 (2008).
- ¹³X.-J. Chen, V. V. Struzhkin, Y. Song, A. F. Goncharov, M. Ahart, Z. Liu, K.-K. Mao, and R. J. Hemley, *Proc. Natl. Acad. Sci. U.S.A.* **105**, 20 (2008).
- ¹⁴X.-J. Chen, J.-L. Wang, V. V. Struzhkin, H.-K. Mao, R. J. Hemley, and H.-Q. Lin, *Phys. Rev. Lett.* **101**, 077002 (2008).
- ¹⁵T. A. Strobel, M. Somayazulu, and R. J. Hemley, *Phys. Rev. Lett.* **103**, 065701 (2009).
- ¹⁶S. Wang, H.-K. Mao, X.-J. Chen, and W. L. Mao, *Proc. Natl. Acad. Sci. U.S.A.* **106**, 14763 (2009).
- ¹⁷G. Kresse and J. Furthmüller, *Comput. Mater. Sci.* **6**, 15 (1996).
- ¹⁸G. Kresse and D. Joubert, *Phys. Rev. B* **59**, 1758 (1999).
- ¹⁹J. P. Perdew, K. Burke, and M. Ernzerhof, *Phys. Rev. Lett.* **77**, 3865 (1996).
- ²⁰W. Tang, E. Sanville, and G. Henkelman, *J. Phys.: Condens. Matter* **21**, 084204 (2009); E. Sanville, S. D. Kenny, R. Smith, and G. Henkelman, *J. Comput. Chem.* **28**, 899 (2007).
- ²¹P. Giannozzi, S. Baroni, N. Bonini, M. Calandra, R. Car, C. Cavazzoni, D. Ceresoli, G. L. Chiarotti, M. Cococcioni, I. Dabo, A. D. Corso, S. d. Gironcoli, S. Fabris, G. Fratesi, R. Gebauer, U. Gerstmann, C. Gougoussis, A. Kokalj, M. Lazzeri, L. Martin-Samos, N. Marzari, F. Mauri, R. Mazzarello, S. Paolini, A. Pasquarello, L. Paulatto, C. Sbraccia, S. Scandolo, G. Sclauzero, A. P. Seitsonen, A. Smogunov, P. Umari, and R. M. Wentzcovitch, *J. Phys.: Condens. Matter* **21**, 395502 (2009).
- ²²S. K. Sharma, H.-k. Mao, and P. M. Bell, *Phys. Rev. Lett.* **44**, 886 (1980).
- ²³N. W. Ashcroft, *Phys.* **2**, 65 (2009).
- ²⁴C. J. Pickard and R. J. Needs, *Nat. Phys.* **3**, 473 (2007).
- ²⁵M. Somayazulu, P. Dera, A. F. Goncharov, S. A. Gramsch, P. Liermann, W. Yang, Z. Liu, H.-k. Mao, and R. J. Hemley, *Nat. Chem.* **2**, 50 (2010).
- ²⁶K. A. Johnson and N. W. Ashcroft, *Nature (London)* **403**, 632 (2000).
- ²⁷C. F. Richardson and N. W. Ashcroft, *Phys. Rev. Lett.* **78**, 118 (1997).
- ²⁸M. Ramzan, S. Lebégue, and R. Ahuja, *Phys. Rev. B* **81**, 233103 (2010).